Mathematical representation and experimental generation of cylindrical vector beams

Tao Duan (段 弢)*, Pengcheng Jin (金鹏程), and Chunfang Li (李春芳)

State Key Laboratory of Transient Optics and Photonics, Xi'an Institute of Optics and Precision Mechanics, Chinese Academia of Sciences, Xi'an 710119, China

**Corresponding author: duantao@opt.ac.cn*

Received December 14, 2010; accepted January 21, 2011; posted online June 27, 2011

Cylindrical vector beams are described by the representation formalism of finite electromagnetic beams in free space. This is achieved by factorizing the field vector into a mapping matrix and a Jones-like vector. The vectorial property of a finite beam can be described by a degree of freedom of the mapping matrix that can be determined by the azimuthal angle of a fixed unit vector with respect to the wave vector. In addition, it is a simple and flexible experimental device for converting linearly polarized light beams into cylindrical vector beams. The radially or azimuthally polarized beam is easily converted into either one of these by varying the applied voltage.

OCIS codes: 230.3720, 260.5430, 120.5060.
doi: 10.3788/COL201109.S10602.

Polarization is one of the fundamental characteristics of a laser beam[1,2]. Most past research has dealt with spatially homogeneous states of polarization, such as linear, elliptical, and circular polarizations. In these cases, the state of polarization does not depend on the spatial location in the beam cross section. However, the inhomogeneous state of polarization has been investigated only in recent years[3−7]. The cylindrical vector (CV) beam, which obeys cylindrical symmetry in both amplitude and polarization, has attracted increasing attention[8]. The radially and azimuthally polarized beams as two basis states of CV beams have been generated using various methods[9−19]. Polarization propagation and interaction with materials have been extensively explored in optical inspection and metrology, display technologies, data storage, optical communications, materials sciences, biological studies, astronomy, and terahertz technology.

The CV beam is the finite electromagnetic wave in free space. As for a finite beam, the state of polarization is not a global property. Rather, it is local and changes upon propagation[20]. Recently, Li advanced a characteristic[21] represented by a unit vector $\boldsymbol{I}$ and found that this symmetry axis was a global property and, together with the Jones vector of the angular spectrum, could describe the vectorial property of a beam. In this letter, we analyze perpendicular $\boldsymbol{I}$ to the propagation axis corresponding to the uniformly polarized beam in the paraxial approximation, and a parallel $\boldsymbol{I}$ to the propagation axis corresponding to the CV beam, including the radially and azimuthally polarized beams. Since 1972[22], various methods for generating CV beams have been developed. Linearly polarized light can be locally rotated to the desired spatial polarization pattern using a device with twisted nematic liquid crystal (LC)[23,24]. In this letter, the device is a simple and flexible experimental tool for converting linearly polarized light beams into CV beams through a liquid crystal polarization converter (LCPC). The radially or azimuthally polarized beam is easily converted into either one of these by varying the applied voltage. Meanwhile, the interaction of the vector beams with materials also leads to other effects such as the spin Hall effect of light[25−29], a transverse displacement of a reflected or a transmitted beam taking place at a dielectric interface. Such phenomenon pertains to the description of the vectorial property of a finite beam.

In a source-free position space, the electric-field vector $\boldsymbol{F}(\boldsymbol{x})$ of a monochromatic finite electromagnetic beam satisfies the transversality condition[21]. In a source-free position space, the finite electric-field vector takes the following factorized form:

$$\mathbf{F}(\mathbf{x}) = \mathrm{M}(\mathbf{x})\boldsymbol{\alpha}, \tag{1}$$

$$M(\mathbf{x}) = \frac{1}{2\pi}\iint mf\exp(\mathrm{i}\boldsymbol{k}\cdot\boldsymbol{x})\mathrm{d}k_x\mathrm{d}k_y, \tag{2}$$

where $\boldsymbol{\alpha} = (\alpha_\mathrm{p}\ \alpha_\mathrm{s})^\mathrm{T}$; $\mathrm{m} = (\mathbf{p}\ \mathbf{s})$, $\sigma = -\mathrm{i}\,(\alpha_\mathrm{p}^*\alpha_\mathrm{s} - \alpha_\mathrm{s}^*\alpha_\mathrm{p})$; $\boldsymbol{\alpha}$ is the normalized Jones-like vector describing the polarization state of the angular spectrum; α_p and α_s denote complex numbers satisfying the normalization condition, $|\alpha_\mathrm{p}|^2 + |\alpha_\mathrm{s}|^2 = 1$; σ represents the polarization ellipticity; and $\mathrm{M}(\mathbf{x})$ is the mapping matrix (MM) for the beam that is determined by the local MM of wave vector space, m. Thus, the field vector in position space is the result of the mapping of the normalized Jones-like vector by the MM.

The unit vectors $\mathbf{p}$ and $\mathbf{s}$ are defined from wave vector $\mathbf{k}$ in terms of an arbitrary fixed real unit vector $\mathbf{I}$ as $\mathbf{p} = \mathbf{s}\times\frac{\mathbf{k}}{k}$, $\mathbf{s} = \dfrac{\mathbf{k}\times\mathbf{I}}{|\mathbf{k}\times\mathbf{I}|}$. The unit vectors $\mathbf{p}$ and $\mathbf{s}$ are satisfied,

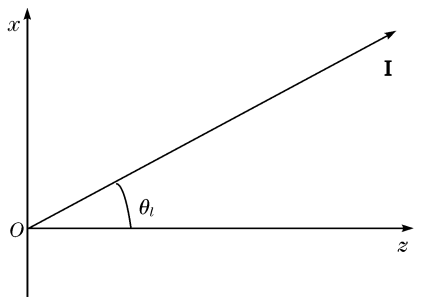

Fig. 1. Unit vector $\mathbf{I}$ in the xoz plane.

$|\mathbf{p}| = |\mathbf{s}| = 1$, $\mathbf{p}\cdot\mathbf{s}=\mathbf{p}\cdot\mathbf{k} = \mathbf{s}\cdot\mathbf{k} = 0$.

Assume that the fixed unit vector $\mathbf{I}$ that is common to all the plane-wave components lies in the plane zox and creates an angle θ_{I} with the z axis (Fig. 1), the propagation axis has

$$\mathbf{I}(\theta_{\mathrm{I}}) = \mathbf{e}_z \cos\theta_I + \mathbf{e}_x \sin\theta_I, \tag{3}$$

so that the MM of the plane-wave component takes the form

$$m = \frac{1}{k|\mathbf{k}\times\mathbf{I}|} \begin{pmatrix} (k_y^2+k_z^2)\sin\theta_I - k_z k_x \cos\theta_I & kk_x\cos\theta_I \\ -k_y(k_x\sin\theta_I + k_z\cos\theta_I) & k(k_z\sin\theta_I - k_x\cos\theta_I) \\ (k_y^2+k_x^2)\cos\theta_I - k_z k_x\sin\theta_I & -kk_y\sin\theta_I \end{pmatrix}, \tag{4}$$

where $|\mathbf{k}\times\mathbf{I}| = [k^2 - (k_x\sin\theta_I + k_z\cos\theta_I)^2]^{1/2}$.

In a circular cylindrical system with the z axis being the symmetry axis, the integral Eq. (2) is changed into

$$\mathrm{M}(\mathbf{x}) = \frac{1}{2\pi}\int_{\mathrm{o}}^{k}\int_{\mathrm{o}}^{\pi} \mathrm{m}f\exp(\mathrm{i}k\cdot\mathrm{x})k_\rho dk_\rho d\varphi. \tag{5}$$

The scalar amplitude of the angular spectrum includes the phase index $\exp(\mathrm{i}l\varphi)$

$$f(k_\rho,\varphi) = f_l(k\rho)\exp(\mathrm{i}l\varphi), \tag{6}$$

where l is an integer. From Eq. (4), we discuss the polarized state of the electric field vector when the unit vector $\mathbf{I}$ is respectively perpendicular or paralled to the propegation axis.

1) unit vector $\mathbf{I}$ perpendicular to the propagation axis:

$$\theta_I = \frac{\pi}{2}, m = \frac{1}{k(k^2-k_z^2)^{\frac{1}{2}}}\begin{bmatrix} (k^2-k_x^2) & 0 \\ -k_x k_y & kk_z \\ -k_z k_x & -kk_y \end{bmatrix}. \tag{7}$$

By applying the paraxial approximation, $\frac{k_x}{k}, \frac{k_y}{k}$ can be regarded as a small number in comparison with unity, then $m = \begin{pmatrix} 1 & 0 \\ 0 & 1 \\ 0 & 0 \end{pmatrix}$.

The longitudinal component is zero. At this time, m is independent of the wave vector and represents the uniform state of polarization beams, the electric-field vector as

$$\mathbf{F}(x) = (\alpha_p\mathbf{e}_x + \alpha_s\mathbf{e}_y)F(r,z)\exp(il\varphi), \tag{8}$$

where

$$F(r,z) = i^{|l|}\int_0^k f_l(k_\rho)\exp(\mathtt{i}k_z z)J_{|l|}(rk_\rho)k_\rho dk^\rho, \tag{9}$$

$\boldsymbol{\alpha} = (a_s \quad a_p)$ is the traditional Jones vector, where the different distribution functions $f_l(k_\rho)$ represent the different electric-field distribution $F(r,z)$. For example, the modified Bessel-Gaussian beam is shown in Fig. 2.

Fundamental Gaussian beams ($l = 0$) and doughnut beams ($\mathrm{l} \neq 0$) can be also obtained:

$$f_l(k_\rho) = (w_0 k_\rho)^{|l|}\exp\left(\frac{-w_o^2}{2}k_\rho^2\right). \tag{10}$$

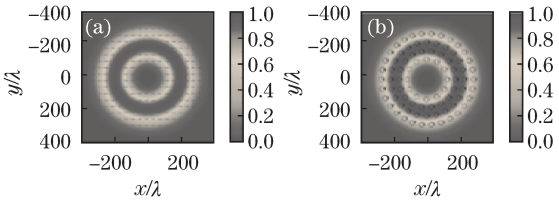

Fig. 2. Modified Bessel-Gaussian beams.

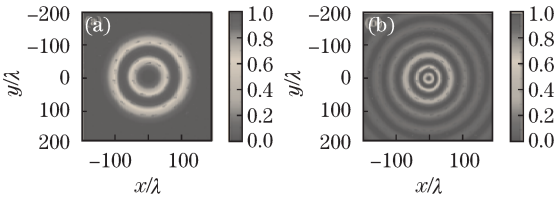

Fig. 3. (a) Bessel-Gaussian beam and (b) Laguerre-Gaussian beam.

2) unit vector $\mathbf{I}$ parallel to the propagation axis:

$$\theta_I = 0, \quad m = \begin{pmatrix} (k^2-k_x^2) & 0 \\ -k_x k_y & k_z \\ -k_z k_x & -kk_y \end{pmatrix} = \left(\frac{k_z}{k}\mathbf{e}_{\mathrm{p}} \;\; -\frac{k\rho}{k}\boldsymbol{e}_{\mathrm{z}} \;\; e_\phi\right). \tag{11}$$

In the paraxial approximation, Eq. (11) turns into $m = (\mathbf{e}_\rho \;\; \mathbf{e}_\varphi)$

Assume that l=0,

$$\mathbf{F}(x) = (\alpha_{\mathrm{p}}\mathbf{e}_r + \alpha_s\mathbf{e}_\varphi)F(r,z), \tag{12}$$

where

$$F(r,z) = \mathrm{i}\int_0^k f_0(k_\rho)\exp(\mathrm{i}k_z z)J_1(rk_\rho)k_\rho dk_\rho. \tag{13}$$

Equation (12) is the CV beam; $\alpha = (1\;\;0)^{\mathrm{T}}$ and $\alpha = (0\;\;1)^{\mathrm{T}}$ are the radial and azimuthal polarized beams, respectively. Figure 3 shows that electric-field distribution $F(r,z)$ when distribution functions $f_0(k_\rho)$ take the shape of Bessel-Gaussian and Laguerre-Gaussian.

A radially polarized or an azimuthally polarized beam, which consists of a variable phase shifter (VPS), polarization rotator (PR), and liquid crystal cell (L-cell), was produced using an LCPC (ARCoptix S. A), as shown in Fig. 4(a)①. The reorientation of the polarization orientation in these polarization converters was due to the twisted nematic effect of the L-cell. As a result, linearly polarized light is typically used as input and then locally rotated to the desired spatial polarization pattern with axial symmetry. Symmetry axis is the propagation axis. Radially and azimuthally polarized light beams are achieved respectively for light incident perpendicular and parallel to the cell axis. However, as shown in Fig. 4(b), the L-cell is separated in the upper and lower parts by the cell axis because of the defect line in the center. On the top half, the rotation of the nematic cell is clockwise, whereas the lower part is characterized by counterclockwise rotation. In this case, the VPS allows for compensation of the $\lambda/2$ phase step between the upper and the lower halves of the L-cell when 1.34-V power is supplied. PR is capable of rotating the entrance po-

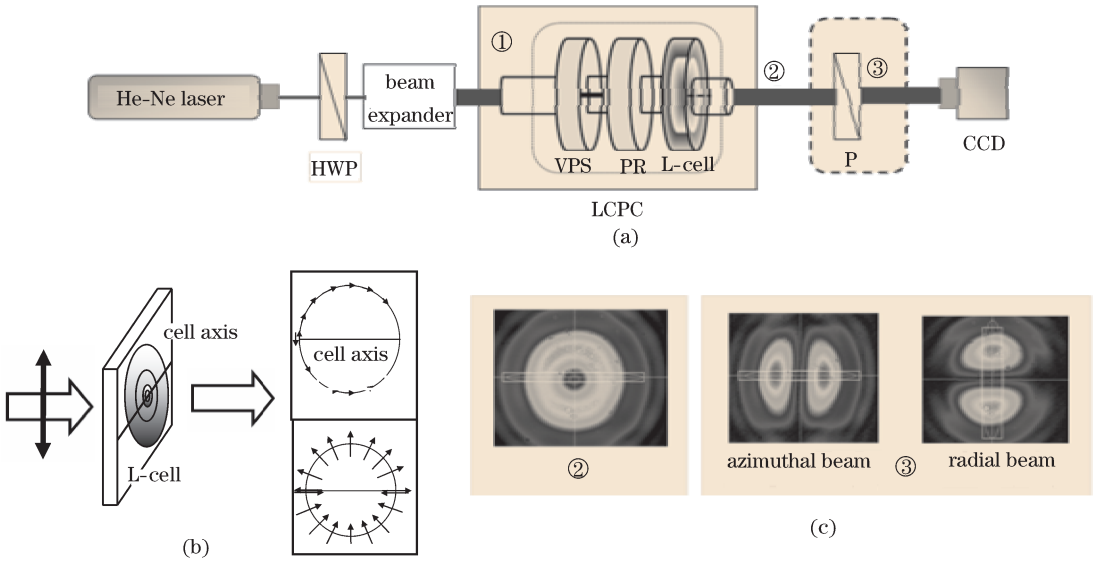

Fig. 4. (a) Schematic of experimental setup for generating radial and azimuthal polarization beams with the LCPC in ①. (b) Spatially variant polarization rotation by the twisted nematic L-cell(upper and lower parts are separated by cell axis in the center of L-cell). (c) ② Without polarizer, for the radially or azimuthally polarized beam; ③ after passing through the analyzing polarizer in the perpendicular direction.

larization by $\pi/2$ and is the switch between the radial and azimuthal polarization distribution by varying the applied voltage.

The schematic of the experimental setup for generating the radial and azimuthal polarization beam is illustrated in Fig. 4(a). The optical source was a collimated He–Ne laser with a wavelength of 632.8 nm and linear polarization. An expanding beam generated by a beam expander and vibration direction of the linearly polarized beam was rotated by the half wavelength plate. Through the polarization converter, a radial polarized beam is produced with the electric field pointing in the radial direction with respect to the optical axis of the beam. In the end, the profile of the beam in Fig. 4(c) was observed by a charge coupled device. The beam becomes a hollow beam, as shown in Fig. 4(c)②, because of the singularity of the polarization at the center. To validate the radial or azimuthal polarization, we placed a polarizer (P) after the liquid crystal polarization converter and found that the intensity is zero in the direction perpendicular or parallel to the polarization axis of the polarizer. The intensity distribution is shown in Fig. 4(c)③. When the polarizer P is rotated, the direction of zero intensity also rotates and is constantly perpendicular to the polarization axis of the polarizer. At the same time, we can easily obtain the azimuthal polarization beam when a bias of (at least) 5 V voltage is applied to the PR.

In conclusion, CV beams are described by the representation formalism of finite electromagnetic beams. This is achieved by factorizing the field vector of a plane wave into a mapping matrix and a Jones-like vector, and investigating the degree of freedom of the MM that corresponds to the direction of the fixed unit vector **I**. Meanwhile, when unit vector **I** is parallel to the propagation, the finite electromagnetic vector field depicts the CV beam, which obeys cylindrical symmetry in both amplitude and polarization axis. In addition, a simple and flexible experimental device is introduced to generate the radially and azimuthally polarized beams using an LCPC. The radially or azimuthally polarized beam is easily converted into either one of these by varying the applied voltage.

This work was supported by the National Natural Science Foundation of China (Nos. 60907026, 60877055, and 60806041).

References

1. M. Born and E. Wolf, *Principles of Optics: Electromagnetic Theory of Propagation, Interference and Diffraction of Light* (Cambridge Univ. Press, 1999).
2. D. H. Goldstein and E. Collett, *Polarized Light* (Marcel Dekker, 2003).
3. Z. Bomzon, M. Gu, and J. Shamir, Appl. Phys. Lett. **89,** 241104 (2006).
4. K. Lindfors, A. Priimagi, T. Setala, A. Shevchenko, A. T. Friberg, and M. Kaivola, Nat. Photonics **1,** 228 (2007).
5. J. Serna and G. Piquero, Opt. Commun. **282,** 197 (2009).
6. T. Wang and J. X. Pu, Opt. Commun. **281,** 3617(2008).
7. Y. Xin, Y. R. Chen, and Q. Zhao, Opt. Commun. **282,** 1260 (2009).
8. D. G. Hall, Opt. Lett. **21,** 9 (1996).
9. M. Stalder and M. Schadt, Opt. Lett. **21,** 1948 (1996).
10. G. Machavariani, Y. Lumer, I. Moshe, A. Meir, and S. Jackel, Opt. Commun. **281,** 732 (2008).
11. N. Passilly, R. de Saint Denis, K. A.-Ameur, F. Treussart, R. Hierle, and J. F. Roch, J. Opt. Soc. Am. A **22,** 984 (2005).
12. A. Shoham, R. Vander, and S. G. Lipson, Opt. Lett. **31,** 3405 (2006).
13. G. Machavariani, Y. Lumer, I. Moshe, A. Meir, and S. Jackel, Opt. Lett. **32,** 1468 (2007).
14. X. Wang, J. Ding, W. Ni, C. Guo, and H. Wang, Opt.

Lett. **32,** 3549 (2007).
15. P. B. Phua, W. J. Lai, Y. L. Lim, K. S. Tiaw, B. C. Lim, H. H. Teo, and M. H. Hong, Opt. Lett. **32,** 376 (2007).
16. J. L. Li, K. Ueda, M. Musha, A. Shirakawa, and L. X. Zhong, Opt. Lett. **31,** 2969 (2006).
17. S. C. Tidwell, D. H. Ford, and W. D. Kimura, Appl. Opt. **29,** 2234 (1990).
18. K. J. Moh, X. C. Yuan, J. Bu, R. E. Burge, and B. Z. Gao, Appl. Opt. **46,** 7544 (2007).
19. P. B. Phua and W. J. Lai, Opt. Express **15,** 14251 (2007).
20. D. N. Pattanayak and G. P. Agrawal, Phys. Rev. A **22,** 1159 (1980).
21. C. F. Li, Phy. Rev. A **78,** 063831 (2008)
22. D. Pohl, Appl. Phys. Lett. **20,** 266 (1972).
23. M. Stalder and M. Schadt, Opt. Lett. **21,** 1948 (1996).
24. K. Xu, Y. Yang, Y. He, X. Han, and C. Li, J. Opt. Soc. Am. A **27,** 572 (2010)
25. M. Onoda, S. Murakami, and N. Nagaosa, Phys. Rev. Lett. **93,** 083901 (2004).
26. K. Y. Bliokh and Y. P. Bliokh, Phys. Rev. Lett. **96,** 073903 (2006).
27. O. Hosten and P. Kwiat, Science **319,** 787 (2008).
28. F. I. Fedorov, Dokl. Akad. Nauk SSSR **105,** 465(1955).
29. F. Pillon, H. Gilles, and S. Girard, Appl. Opt. **43,** 1863 (2004).